Nano Active Stabilization System - Introduction

Dehaeze Thomas

May 30, 2024

Contents

1 Context of this thesis

1.1 Synchrotron Radiation Facilities

Accelerating electrons to produce intense X-ray

- Explain what is a Synchrotron: light source
- Say how many there are in the world (~50). The main ones are shown in Figure 1.1.

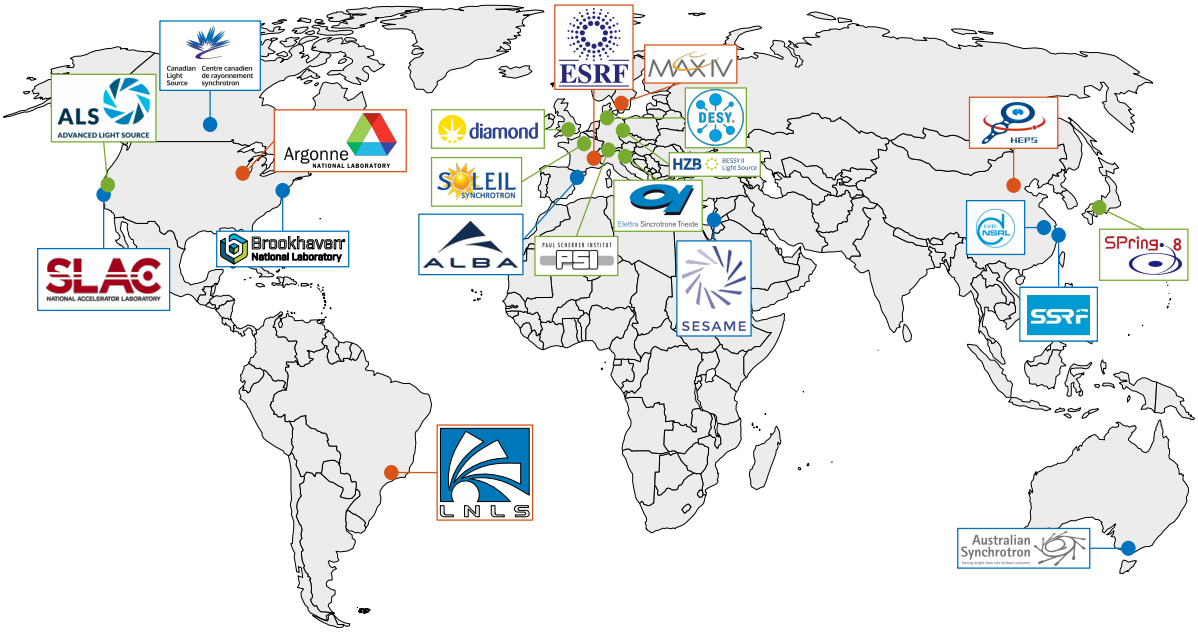

Figure 1.1: Major synchrotron radiation facilities in the world. 3rd generation Synchrotrons are shown in blue. Planned upgrades to 4th generation are shown in green, and 4th generation Synchrotrons in operation are shown in red.

- Electron part: LINAC, Booster, Storage Ring 1.2a
- Synchrotron radiation: Insertion device / Bending magnet
- Many beamlines (large diversity in terms of instrumentation and science)
- Science that can be performed:
  - structural biology, structure of materials, matter at extreme, ...

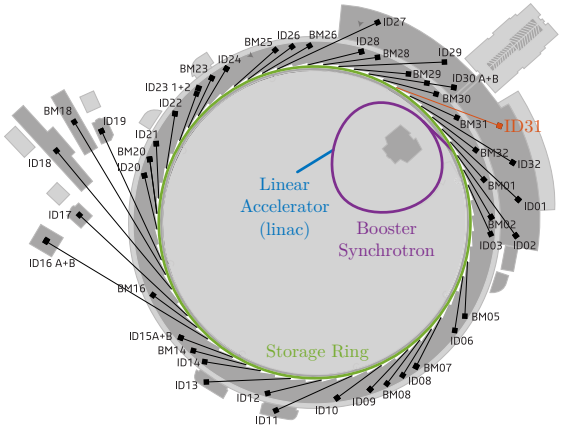

(a) Schematic of the ESRF. The linear accelerator is shown in blue, the booster synchrotron in purple and the storage ring in green. There are over 40 beamlines, the ID31 beamline is highlighted in red

(b) European Synchrotron Radiation Facility

Figure 1.2: Schematic (a) and picture (b) of the European Synchrotron Radiation Facility

The European Synchrotron Radiation Facility

3rd and 4th generation Synchrotrons Brilliance: figure of merit for synchrotron

- 4th generation light sources [1]

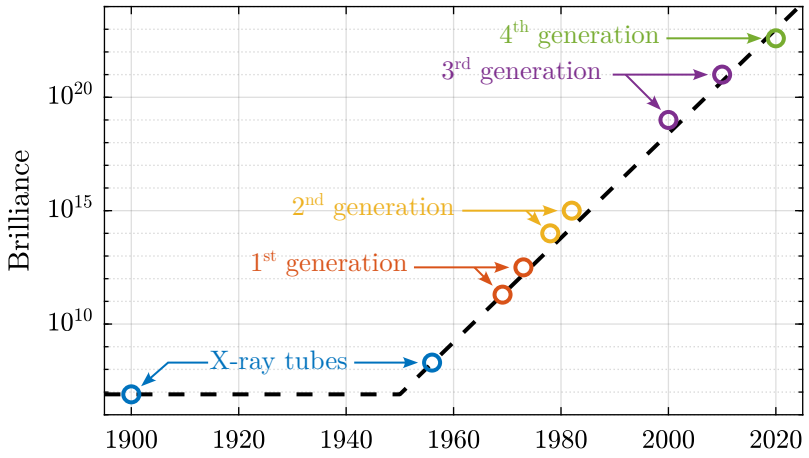

Figure 1.3: Evolution of the peak brilliance (expressed in photons/$s/mm^2/mrad^2/0.1\%BW$) of synchrotron radiation facilities. Note the vertical logarithmic scale.

1.2 The ID31 ESRF Beamline

Beamline Layout

- General layout: source (insertion device), optical hutches (OH1, OH2), experimental hutch (EH)
- Beamline layout (OH Figure 1.4, EH 1.5) All these optical instruments are used to "shape" the x-ray beam as wanted (monochromatic, wanted size, focused, etc…)
- ID31 and Micro Station (Figure 1.5) Check https://www.esrf.fr/UsersAndScience/Experiments/StructMaterials/ID31 https://www.wayforlight.eu/beamline/23244
- X-ray beam + detectors + sample stage
- Focusing optics
- Optical schematic with: source, lens, sample and detector. Explain that what is the most important is the relative position between the sample and the lens.
- Explain the XYZ frame for all the thesis (ESRF convention: X: x-ray, Z gravity up)

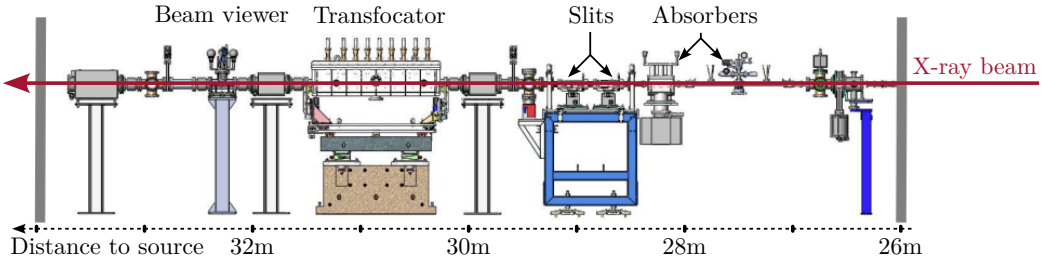

(a) OH1

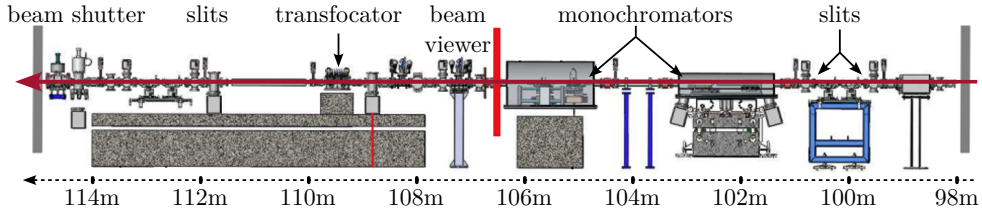

(b) OH2

Figure 1.4: Schematic of the two ID31 optical hutches: OH1 (a) and OH2 (b). Distance from the source (the insertion device) is indicated in meters.

Positioning End Station: The Micro-Station Micro-Station:

- DoF with strokes: Ty, Ry, Rz, Hexapod
- Experiments: tomography, reflectivity, truncation rod, … Make a table to explain the different "experiments"
- Explain how it is used (positioning, scans), what it does. But not about the performances
- Different sample environments

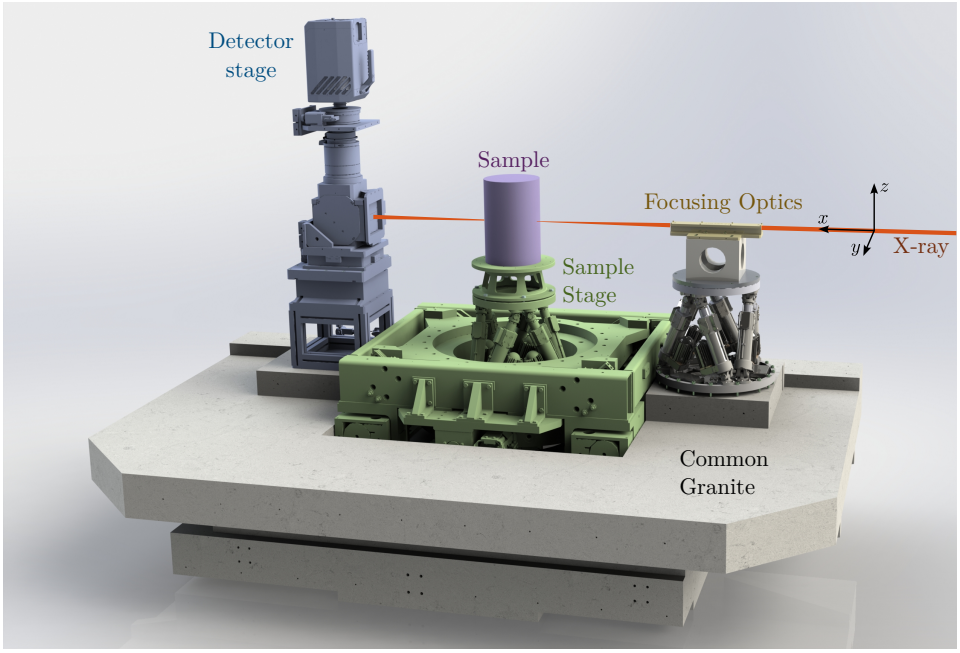

Figure 1.5: CAD view of the ID31 Experimal Hutch (EH). There are typically four main elements: the focusing optics in yellow, the sample stage in green, the sample itself in purple and the detector in blue. All these elements are fixed to the same granite.

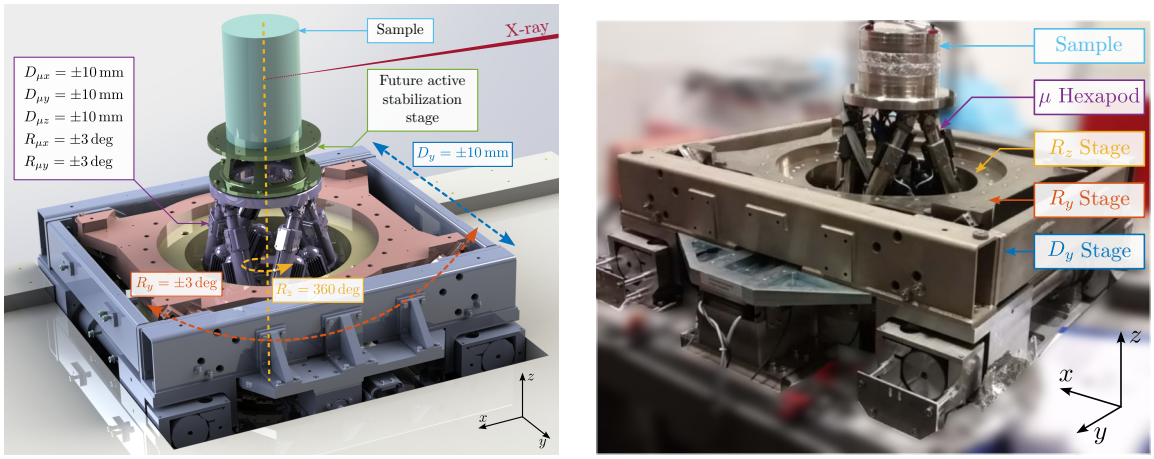

(a) CAD view **(b)** Picture

Figure 1.6: The micro-station. CAD view is shown in (a) with the associated degrees of freedom. A picture of the micro-station is shown in (b) during the assembly process.

Scientific experiments performed on ID31

- Few words about science made on ID31 and why nano-meter accuracy is required
- Typical experiments (tomography, ...), various samples (up to 50kg), sample environments (high temp, cryo, etc..)
  - Alignment of the sample, then
  - Reflectivity
  - Tomography
  - Diffraction tomography: most critical
- Two example:
  - Tomography: compute image as a function of the angle. To reconstruct 3D image, the position has to be known with good accuracy [2]
  - Mapping: focused beam on the sample, 20nm step size, accuracy of the obtained image is directly linked to the beam size and the position accuracy/vibrations [3]

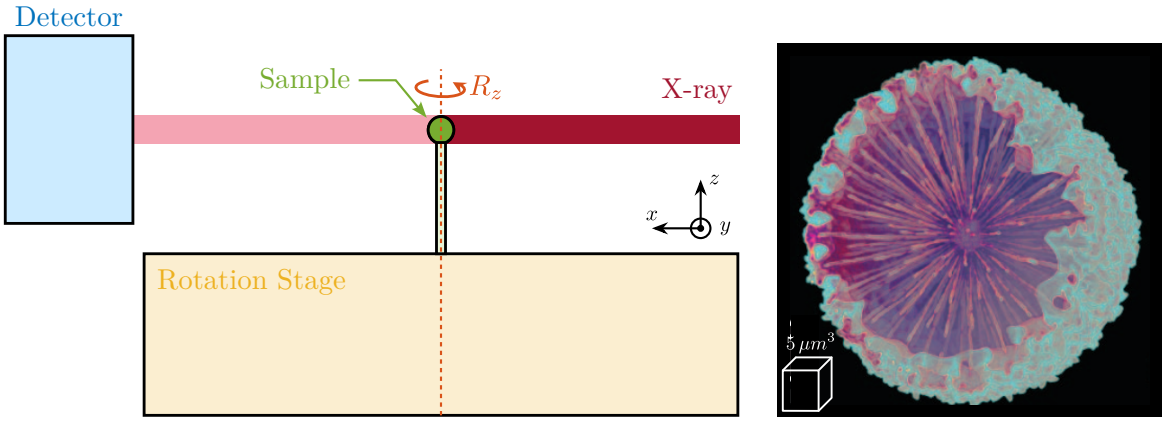

(a) Experimental setup **(b)** Obtained image [2]

Figure 1.7: Exemple of a tomography experiment. The sample is rotated and images are taken at several angles (a). Example of one 3D image obtained after tomography (b).

1.3 Need of Accurate Positioning End-Stations with High Dynamics

A push towards brighter and smaller beams Improvement of both the light source and the instrumentation:

- EBS: smaller source + higher flux 1.9

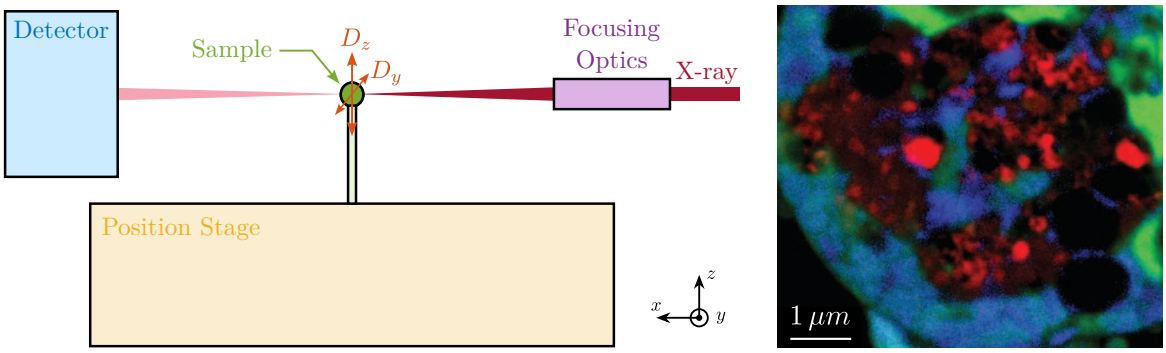

(a) Experimental setup **(b)** Obtained image [3]

Figure 1.8: Exemple of a scanning experiment. The sample is scanned in the Y-Z plane (a). Example of one 2D image obtained after scanning with a step size of 20nm (b).

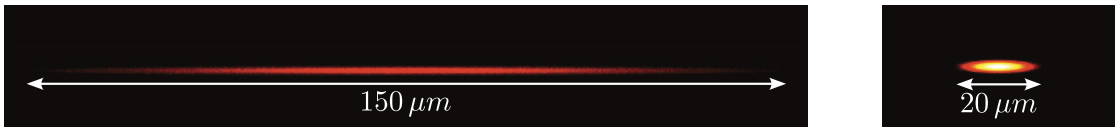

(a) 3^{rd} generation **(b)** 4^{th} generation

Figure 1.9: View of the ESRF X-ray beam before the EBS upgrade (a) and after the EBS upgrade (b). The brilliance is increased, whereas the horizontal size and emittance are reduced.

- ESRF Red Book (1987): very few beamline projects aiming even for 10 micron sized beams Now optics exist for 10nm beams
- Better focusing optic (add some links): beam size in the order of 10 to 20nm FWHM (reference) 1.10 crossed silicon compound refractive lenses, KB mirrors [17], zone plates [18], or multilayer Laue lenses [19] [4]

Higher flux density (+high energy of the ID31 beamline) => Radiation damage: needs to scan the sample quite fast with respect to the focused beam

- Allowed by better detectors: higher sampling rates and lower noise => possible to scan fast [5]

New dynamical positioning needs "from traditional step by step scans to *fly-scan*"

Fast scans + needs of high accuracy and stability => need mechatronics system with:

- accurate metrology
- multi degree of freedom positioning systems
- fast feedback loops

Shift from step by step scan to *fly-scan* [6]

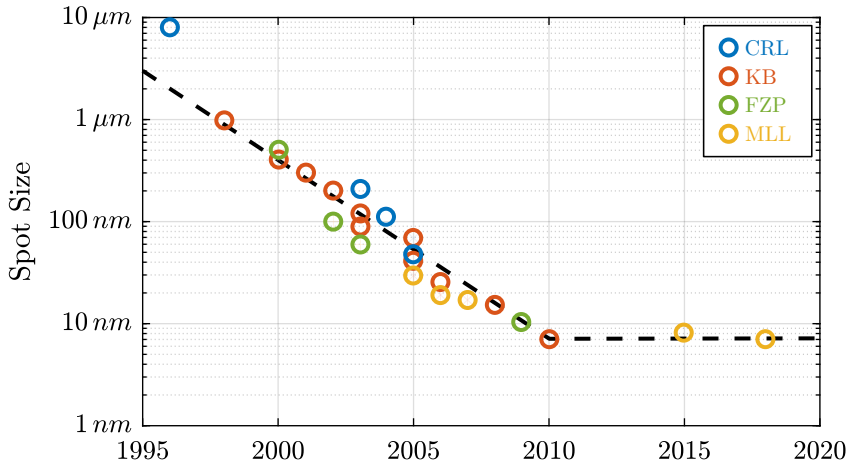

Figure 1.10: Evolution of the measured spot size for different hard x-ray focusing elements. CRL, KB, FZP, MLL

- Much lower pixel size + large image => takes of lot of time if captured step by step. Explain what is step by step scanning: move motors from point A to point B, stops, start detector acquisition, open shutter , close the shutter, move to point C, ...

[7]

> n traditional step scan mode, each exposure position requires the system to stop prior to data acquisition, which may become a limiting factor when fast data collection is required. Fly-scanning is chosen as a preferred solution that helps overcome such speed limitations [5, 6]. In fly-scan mode, the sample keeps moving and a triggering system generates trigger signals based on the position of the sample or the time elapsed. The trigger signals are used to control detector exposure.

Subject of this thesis: design of high performance positioning station with high dynamics and nanometer accuracy

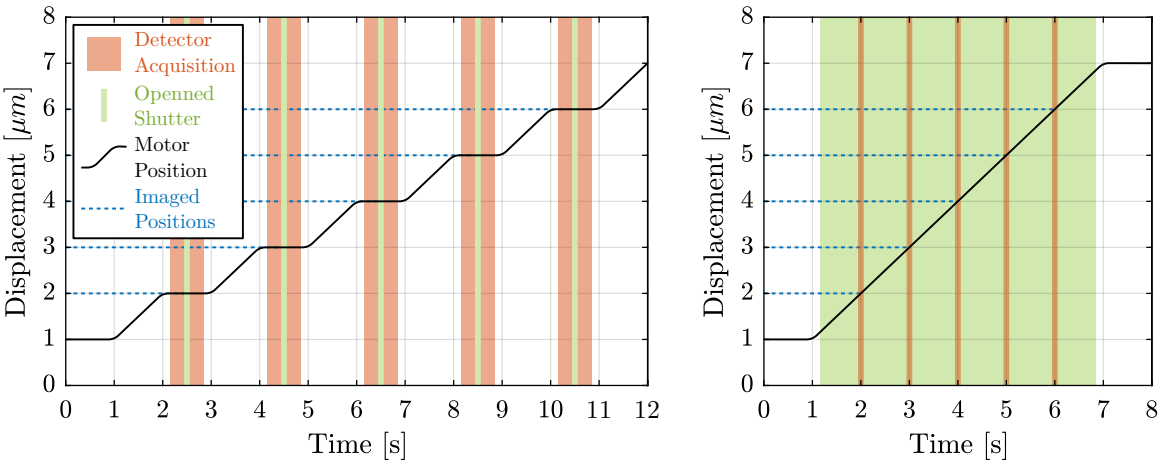

(a) Step by step scan

(b) Fly scan

Figure 1.11: Two acquisition modes. In step-by-step mode (a), the motor moves at the wanted imaged position, the detector acquisition is started, the shutter is openned briefly to have the wanted exposition, the detector acquisition is stopped, and the motor can move to a new position. In *fly-scan* mode (b), the shutter is openned during all the motion, and the detector is acquired only at the wanted positions, on the *fly*.

2 Challenge definition

2.1 Multi degrees of freedom, long stroke and highly accurate positioning end station

Performance limitation of "stacked-stages" end-stations Typical positioning end station (Figure 2.1):

- stacked stages
- Ball-screw, linear guides, rotary motor

Explain the limitation of performances:

- Backlash, play, thermal expansion, guiding imperfections, ...
- Give some numbers: straightness of the Ty stage for instance, change of 0.1^oC with steel gives x nm of motion
- Vibrations
- Possibility to have linear/rotary encoders that correct the motion in the considered DoF, but does not change anything to the other 5DoF

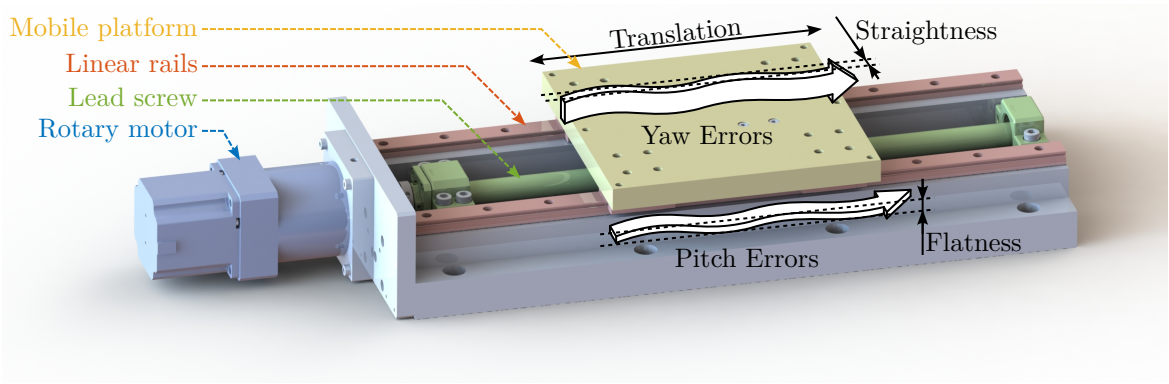

Figure 2.1: A classical translation stage composed of: a rotary motor and possibly reduction gears (in blue), a mechanism to transform the rotary motion to a translation (here a lead screw in green), a guiding mechanism (here linear rails and bearings in red). The mobile platform (in yellow) can then translate with respect to the fixed base.

Flexure based positioning stations may give better positioning requirements, but are limited to short

stroke. Advantages: no backlash, etc… But: limited to short stroke Picture of schematic of one positioning station based on flexure

Explain example of Figure 2.2.

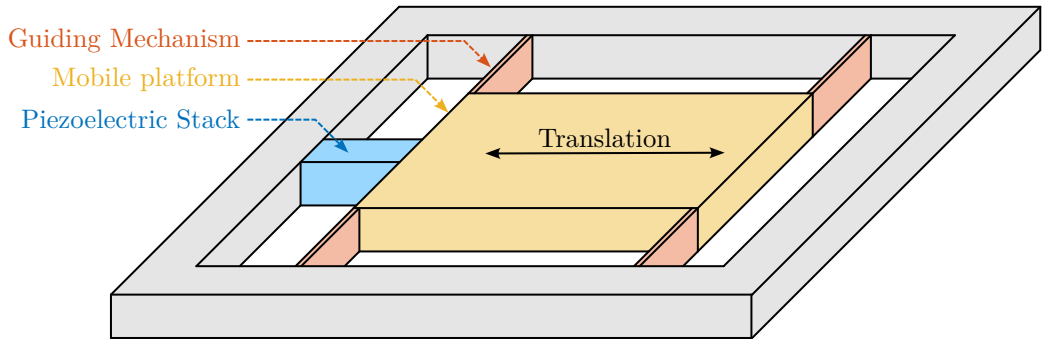

Figure 2.2: A simple flexure stage

Combining, long stroke and accuracy in multi-DoF is challenging.

Positioning accuracy of the ID31 Micro-Station Presentation of the Micro-Station in details 1.6:

- Goal of each stage (e.g. micro-hexapod: static positioning, Ty and Rz: scans, …)
- Stroke
- Initial design objectives: as stiff as possible, smallest errors as possible

Explain that this micro-station can only have ~10um / 10urad of accuracy due to physical limitation.

New positioning requirements

- To benefits from nano-focusing optics, new source, etc… new positioning requirements
- Positioning requirements on ID31:
  - Maybe make a table with the requirements and the associated performances of the micro-station
  - Make tables with the wanted motion, stroke, accuracy in different DoF, etc..
- Sample masses

The goal in this thesis is to increase the positioning accuracy of the micro-station to fulfil the initial positioning requirements.

Goal: Improve accuracy of 6DoF long stroke position platform

2.2 The Nano Active Stabilization System

NASS Concept In order to address the new positioning requirements, the concept of...

Briefly describe the NASS concept. 6DoF vibration control platform on top of a complex positioning platform that correct positioning errors based on an external metrology

It is composed of mainly four elements:

- The micro station
- A 5 degrees of freedom metrology system
- A 5 or 6 degrees of freedom stabilization platform
- Control system and associated instrumentation

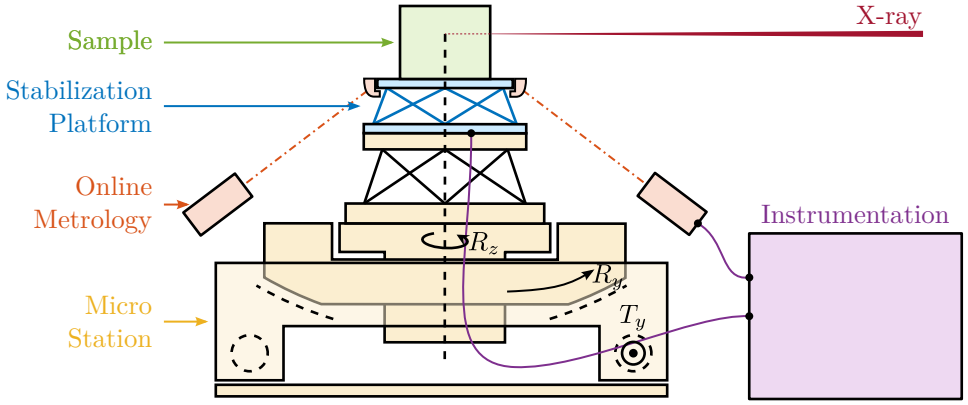

Figure 2.3: The Nano Active Stabilization System concept

Online Metrology system The accuracy of the NASS will only depend on the accuracy of the metrology system.

Requirements:

- 5 DoF
- long stroke
- nano-meter accurate
- high bandwidth

Concept:

- Fiber interferometers
- Spherical reflector with flat bottom

- Tracking system (tip-tilt mechanism) to keep the beam perpendicular to the mirror surface: Spherical mirror with center at the point of interest => No Abbe errors
- XYZ positions from at least 3 interferometers pointing at the spherical surface
- Rx/Ry angles from at least 3 interferometers pointing at the bottom flat surface

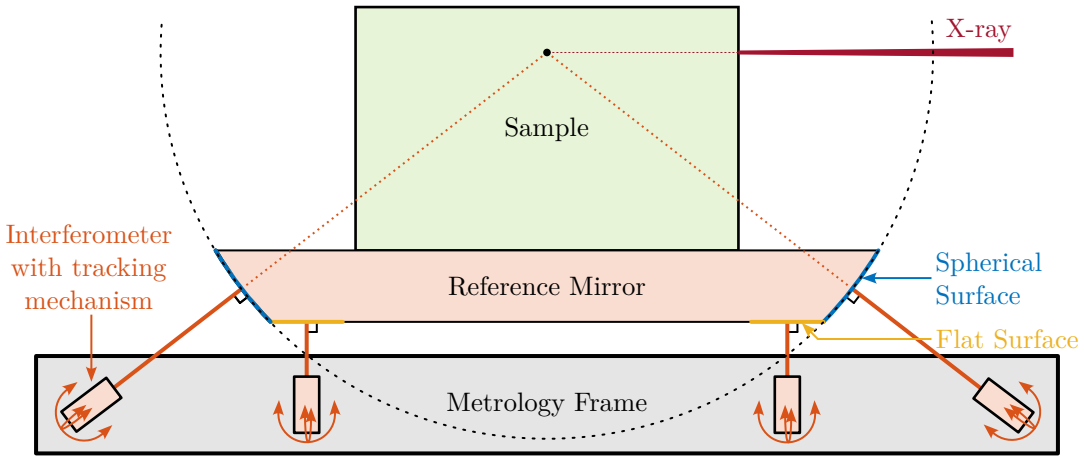

Figure 2.4: 2D representation of the NASS metrology system.

Complex mechatronics system on its own. This metrology system is not further discussed in this thesis as it is still under active development. In the following of this thesis, it is supposed that the metrology system is accurate, etc..

Active Stabilization Platform

- 5 DoF
- High dynamics
- Nano-meter capable (no backlash)
- Accept payloads up to 50kg

MIMO robust control strategies Explain the robustness need?

- 24 7/7 ...
- That is why most of end-stations are based on well-proven design (stepper motors, linear guides, ball bearing, ...)
- Plant uncertainty: many different samples, use cases, rotating velocities, etc...

Trade-off between robustness and performance in the design of feedback system.

2.3 Predictive Design

- The performances of the system will depend on many factors:
  - sensors
  - actuators
  - mechanical design
  - achievable bandwidth
- Need to evaluate the different concepts, and predict the performances to guide the design
- The goal is to design, built and test this system such that it work as expected the first time. Very costly system, so must be correct.
- Challenge:
  - proper design methodology
  - accurate models

2.4 Control Challenge

High bandwidth, 6 DoF system for vibration control, fixed on top of a complex multi DoF positioning station, robust, …

- Many different configurations (tomography, Ty scans, slow fast, …)
- Complex MIMO system. Dynamics of the system could be coupled to the complex dynamics of the micro station
- Rotation aspect, gyroscopic effects, actuators are rotating with respect to the sensors
- Robustness to payload change: very critical. Say that high performance systems (lithography machines, etc…) works with calibrated payloads. Being robust to change of payload inertia means large stability margins and therefore less performance.

3 Literature Review

3.1 Nano Positioning End-Stations

End-Station with Stacked Stages Stacked stages:

- errors are combined

To have acceptable performances / stability:

- limited number of stages
- high performances stages (air bearing etc...)

Examples:

- ID01 [8]
- ID11 [9]
- ID13 [10]

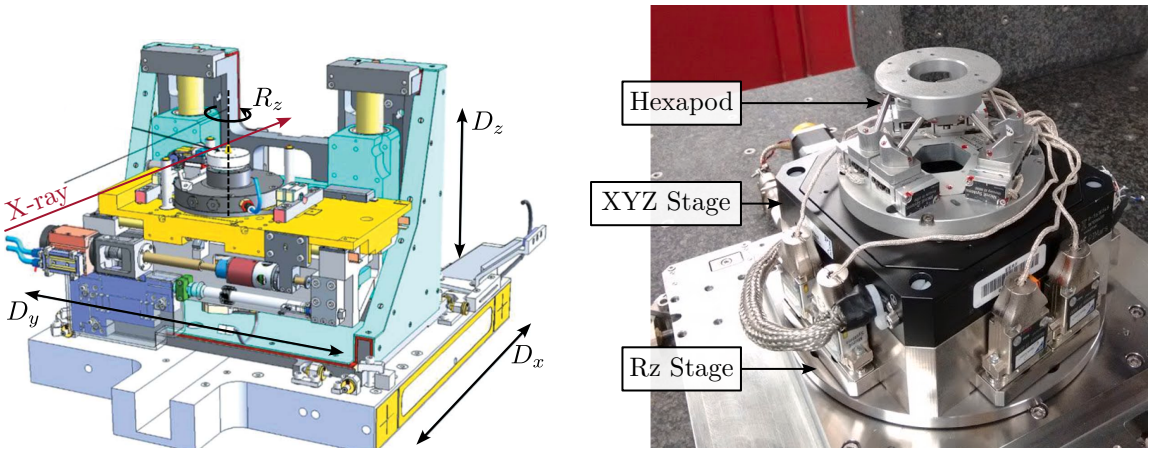

(a) ID16b **(b)** ID11

Figure 3.1: Example of two nano end-stations without online metrology: (a) [11] and (b) [9]

Explain limitations => Thermal drifts, run-out errors of spindles (improved by using air bearing), straightness of translation stages, ...

Online Metrology and Active Control of Positioning Errors The idea of having an external metrology to correct for errors is not new.

Several strategies:

- only used for measurements (post processing)
- for calibration
- for triggering detectors
- for real time positioning control (Figure 3.3)

Sensors:

- Capacitive: [12]–[14]
- Fiber Interferometers Interferometers:
  - Attocube FPS3010 Fabry-Pérot interferometers: [15]–[18]
  - Attocube IDS3010 Fabry-Pérot interferometers: [19]–[21]
  - PicoScale SmarAct Michelson interferometers: [7], [12], [14], [22]

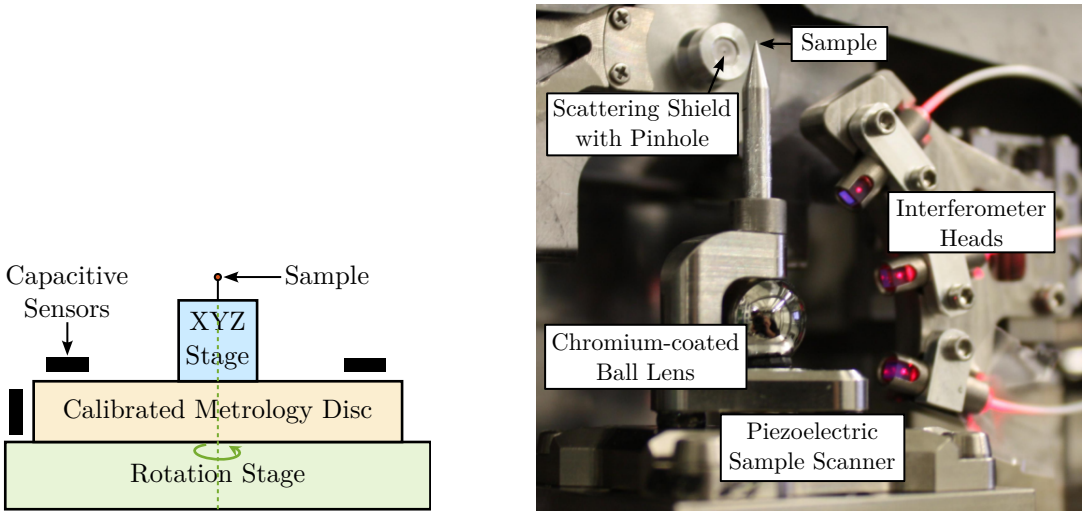

(a) Wang **(b)** Schroer

Figure 3.2: Two examples of end-station with integrated online metrology. (a) [23] and (b) [12]

For some applications (especially when using a nano-beam), the position has not only to be measured, but to be controlled.

Actuators:

- Piezoelectric: [13], [15], [18]–[20]

- 3-phase linear motor: [16], [17]
- Voice Coil: [21], [22]

Bandwidth: rarely specificity. Usually slow, so that only drifts are compensated. Only recently, high bandwidth (100Hz) have been reported with the use of voice coil actuators [21], [22].

Full rotation for tomography:

- Spindle above XYZ stage: [7], [13], [16]–[20]
- Spindle bellow XYZ stage: [12], [14], [22], [23]

Only for mapping: [15], [21]

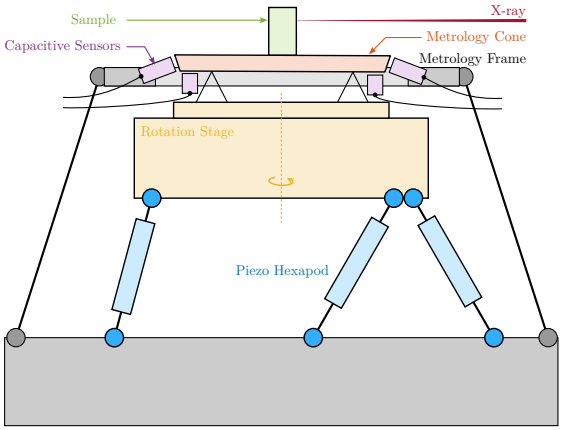

(a) ID16a

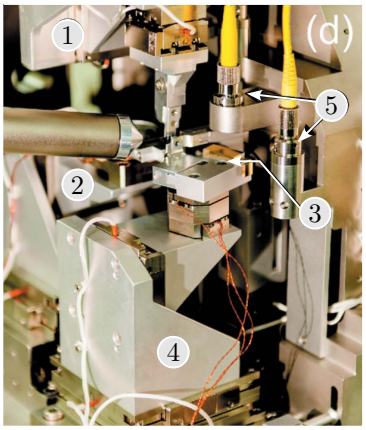

(b) 1 and 2 are stage to position the focusing optics. 3 is the sample location, 4 the sample stage and 5 the interferometers

Figure 3.3: Example of two end-stations with real-time position feedback based on an online metrology. (a) [13]. (b) [15], [24]

Payload capabilities:

- All are only supported calibrated, micron scale samples
- Higher sample masses to up to 500g have been reported in [18], [21]

100 times heavier payload capabilities than previous stations with similar performances.

Long Stroke - Short Stroke architecture Speak about two stage control?

- Long stroke + short stroke
- Usually applied to 1dof, 3dof (show some examples: disk drive, wafer scanner)
- Any application in 6DoF? Maybe new!

Table 3.1: End-Stations with integrated feedback loops based on online metrology. Stages used for static positioning are ommited for readability. Stages used for feedback are indicated in bold font.

Architecture	Metrology	Stroke	Bandwidth	Institute	References
Mirror / Sample **XYZ piezo motors**	3 Interferometers $D_x D_y D_z$	$D_x D_y D_z$: 3 mm		APS	[15] Figure 3.3b
Metrology Ring / Sample Spindle **Piezo Hexapod**	12 Capacitive $D_x D_y D_z R_x R_y$	light R_z : 180 deg $D_x D_y D_z$: 50 μm $R_x R_y$: 500 μrad	10 Hz	ESRF (ID16a)	[13] Figure 3.3a
Spherical Reference / Sample Spindle **Piezo Tripod**	5 Interferometers $D_y D_z R_x$	light R_z : 365 deg $D_x D_y D_z$: 400 μm		PSI (OMNY)	[19], [20]
Cylindrical Reference / Sample Spindle **Stacked XYZ linear motors**	5 Interferometers $D_x D_y D_z R_x R_y$	light R_z : 360 deg $D_x D_y D_z$: 400 μm		Soleil	[16], [17]
Metrology Ring / Sample Spindle **XYZ piezo**	3 Interferometers $D_x D_y D_z$	up to 500g R_z : 360 deg $D_x D_y D_z$: 100 μm		NSLS (SRX)	[18]
Mirrors / Sample **Parallel XYZ voice coil**	3 Interferometers $D_x D_y D_z$	up to 350g $D_x D_y D_z$: 3 mm	100 Hz	Diamond (I14)	[21]
Retroreflectors / Samples **Parallel XYZ voice coil** Spindle	3 Interferometers $D_x D_y D_z$	light $D_y D_z$: 3 mm R_z : $\pm$110 deg	100 Hz	LNLS (Carnauba)	[22]
Sample **Hexapod** Spindle Ry Ty	6 Interferometers $D_x D_y D_z R_x R_y$	**up to 50kg** R_z : 360 deg R_y : $\pm$3 deg D_y : $\pm$5 mm		ESRF (ID31)	[50], [51]

- In the table, say which ones are long stroke / short stroke. Some new stages are just long stroke (voice coil)

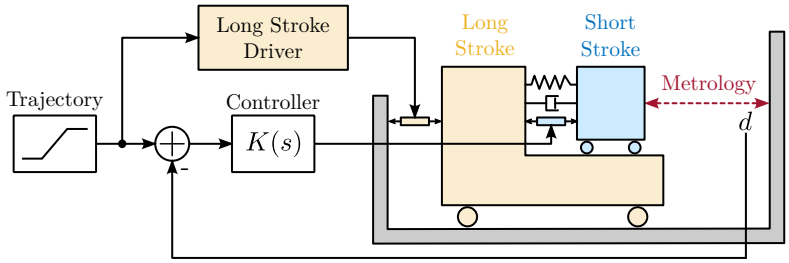

Figure 3.4: Typical Long Stroke - Short Stroke architecture. The long stroke stage is ...

3.2 Multi-DoF dynamical positioning stations

Serial and Parallel Kinematics Example of several dynamical stations:

- XYZ piezo stages
- Delta robot? Octoglide?
- Stewart platform

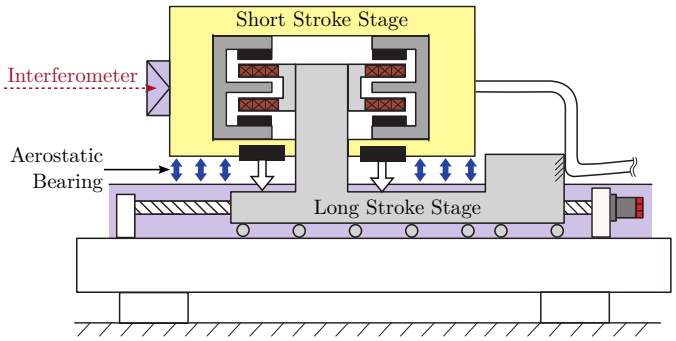

(a) Two stage control with classical stage and voice coil

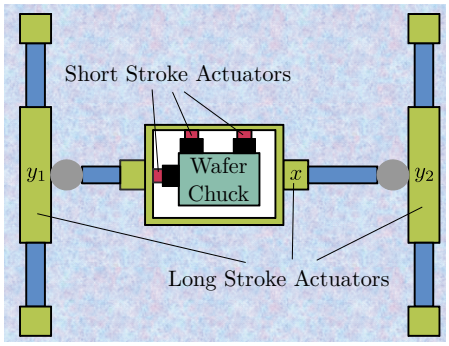

(b) H-bridge. y_1, y_2 and x are 3-phase linear motors. Short stroke actuators are voice coils.

Figure 3.5: (a) [25], (b) [26]

Serial vs parallel kinematics (table?)

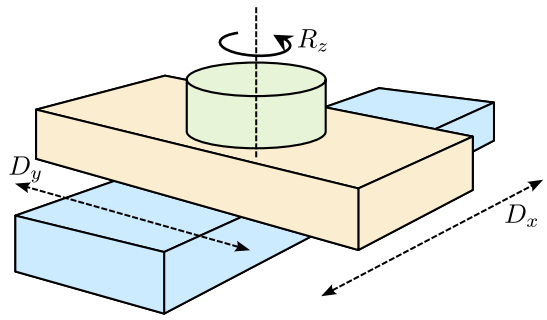

(a) Serial Kinematics

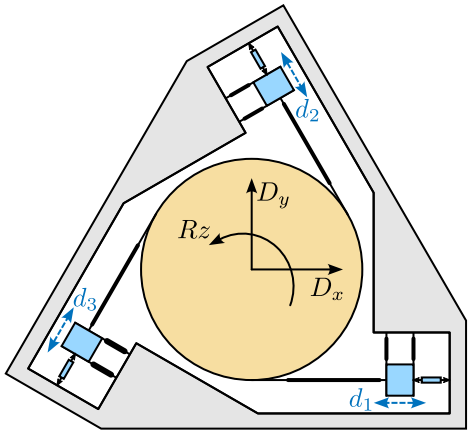

(b) Parallel Kinematics

Figure 3.6: Two positioning platforms with $D_x/D_y/R_z$ degrees of freedom. One is using serial kinematics (a), while the other uses parallel kinematics (b)

Stewart platforms

Explain the normal stewart platform architecture

Make a table that compares the different stewart platforms for vibration control. Geometry (cubic), Actuator (soft, stiff), Sensor, Flexible joints, etc.

3.3 Mechatronics approach

Predicting performances using models [29] Can use several models:

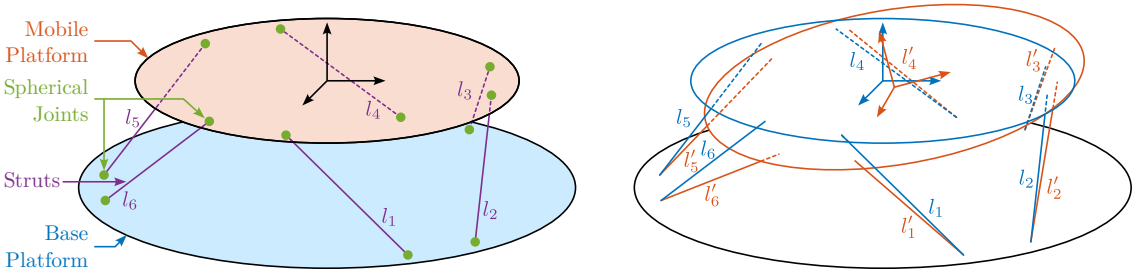

(a) Stewart Platform Architecture

(b) Change of mobile platform pose

Figure 3.7: The Stewart Platform. Architecutre is shown in (a). Change of pose induce by change of strut length is shown in (b)

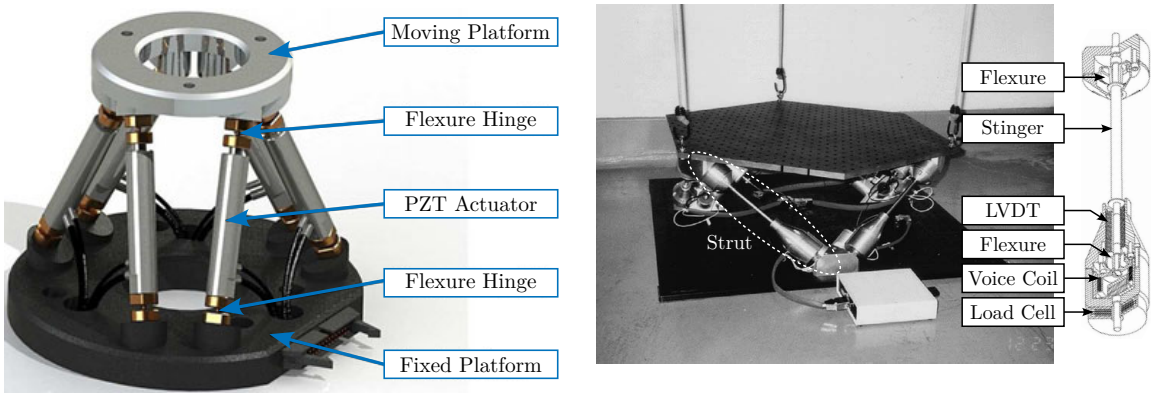

(a) PZT based, for positioning purposes

(b) Voice coil based, Cubic architecture, for vibration isolation

Figure 3.8: Example of Stewart platforms. (a) [27] and (b) [28]

Lumped mass-spring-damper models usually uniaxial, easily put into equations, 1dof per considered mass [30]

Multi-Body Models usually 6dof per considered solid body, some may be constrained using joints

Finite element models Can include FEM into multi-body models: Sub structuring ([31])

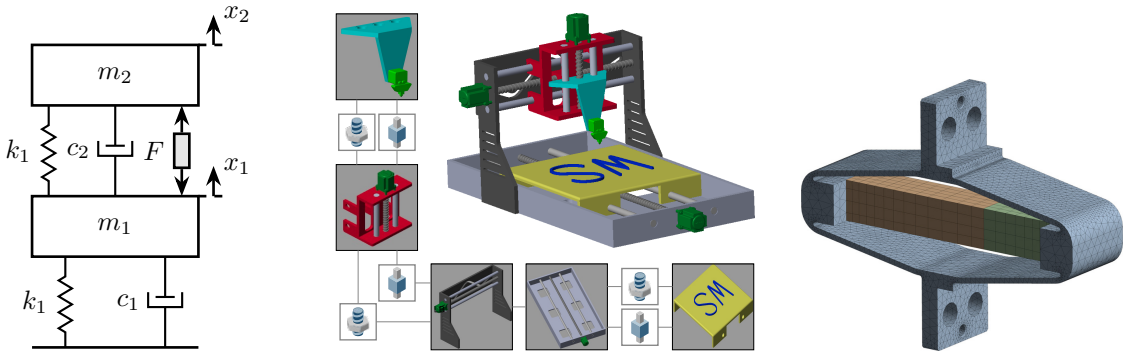

(a) Mass-Spring-Damper model **(b)** Multi-Body model **(c)** Finite Element Model

Figure 3.9: Types of models used when using a mechatronics approach. (a) (b) (c)

Closed-Loop Simulations [26]

Once a model of the system is obtained: develop controller based on linearized model.

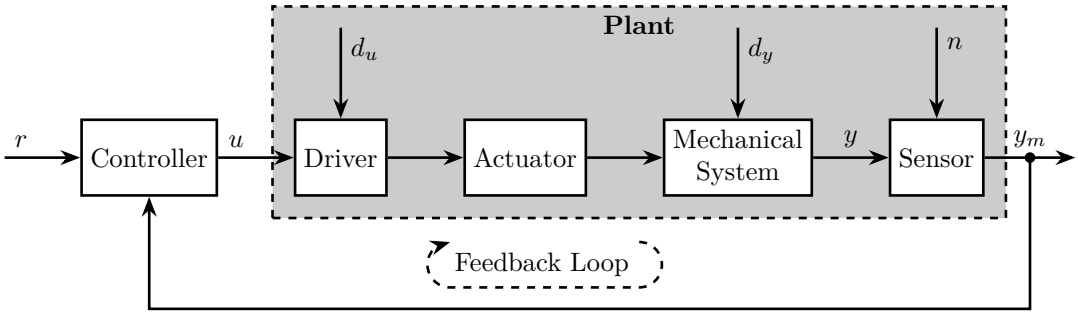

Figure 3.10: Block diagram of a typical feedback control architecture

Say what can limit the performances for a complex mechatronics systems as this one:

- Disturbances affecting the plant output d_y
- Measurement noise n
- DAC / amplifier noise (actuator) d_u
- Feedback system / bandwidth
- r, y_m

Simulations can help evaluate the behavior of the system.

Dynamic Error Budgeting [29] [32]

[33]

- "the disturbance signals are modeled with their power spectral density (PSD), assuming that they are stationary stochastic processes which are not correlated with each other"
- Effects of d_u, d_y and n on y can be estimated from their PSD and the closed-loop transfer functions This gives a first idea of the limiting factor as a function of frequency. In order to determine whether each disturbance/noise impact the performances, cumulative power spectrum can be used: this gives the RMS value Then, this help to know the different actions to improve the performances: reduce sensor noise or driver electrical noise, work on reducing disturbances like damping resonances, increase feedback bandwidth, ...)

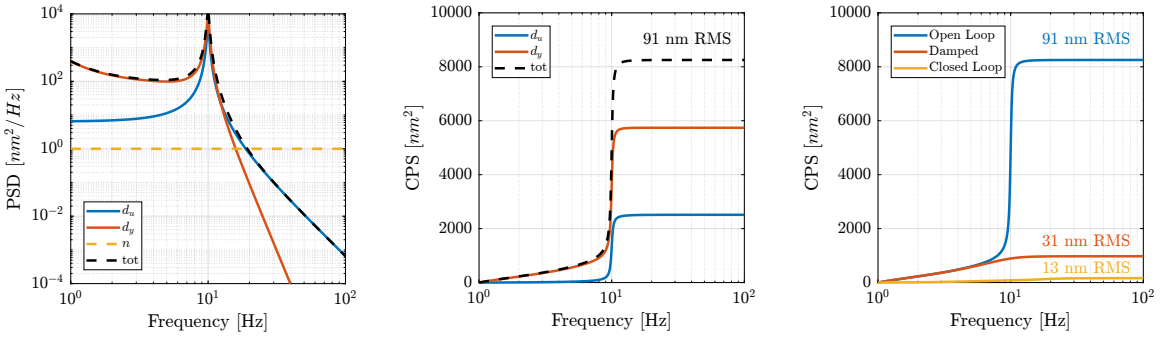

(a) Power Spectral Density - Open Loop **(b)** Cumulative Power Spectrum - Open Loop **(c)** Cumulative Power Spectrum - Comparison

Figure 3.11: Tools used for the dynamic error budgeting. First the Power Spectral Density can be compared (a). The cumulative power spectrum is shown in (b). To compare the effectivness of different strategies, the cumulative power spectrum can be compared (c)

3.4 Stewart platforms: Control architecture

Different control goals:

- Vibration Isolation 3.12a
- Position 3.12b

Depending on the goal, different sensors and different architectures.

For the NASS, both objectives.

Active Damping and Vibration Control Two main active vibration isolation strategies [34]:

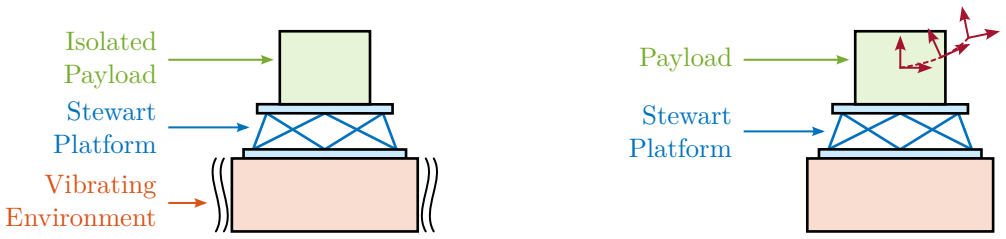

(a) Vibration Isolation **(b)** Positioning

Figure 3.12: Example of two control goals. In (a), the Stewart platform is used to isolate the payload from a vibration environment. In (b), the Stewart platform is used to position the payload along a defined trajectory.

- IFF using collocated force sensors / load cell [35]
- Skyhook damping using inertial sensors (accelerometers, geophones), usually in the frame of the struts

Usually, "decentralized", in the frame of the struts (Figure 3.14). Optimization based on one "strut", and then applied to all the struts simultaneously to obtained a 6-DoF active damping / vibration control system.

If narrow band disturbances: Adaptive feedforward control.

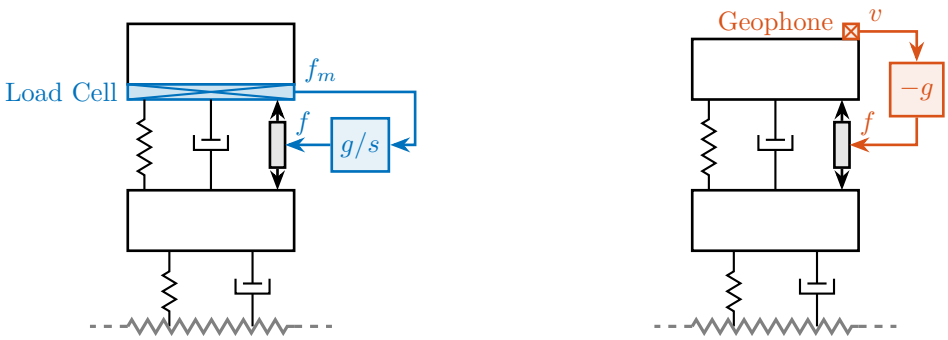

(a) Integral Force Feedback **(b)** "Sky-hook" Damping

Figure 3.13: Uniaxial vibration isolation strategies. Integral force feedback (a) and "sky-hook" damping (b).

Position and Pointing Control Control based on position sensors. Wanted position is generally expressed in the cartesian frame.

Sensors can be:

- In the frame of the struts (LVDT, Encoder, Strain gauges): usually decentralized control (Figure 3.14b)
- External sensors: centralized

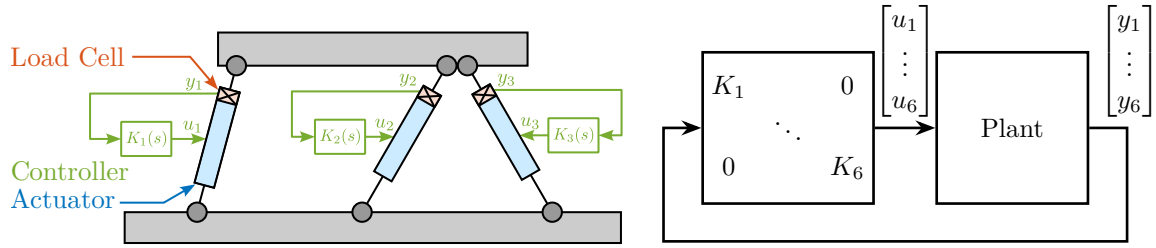

(a) Decentralized Control applied on Stewart platform **(b)** Equivalent block diagram

Figure 3.14: Decentralized control. Example of decentralized force feedback (a), only three struts are shown for simplicity. Equivalent block diagram (b), the controller is then diagonal.

When using external sensors, a decoupling strategy is usually employed (Figure 3.15b):

- Jacobian matrices: frame of the struts or cartesian frame
- Modal control
- Singular Value Decomposition
- Multivariable control: LQG, H-Infinity (Figure 3.15a)

From [36]:

> xperimental closed-loop control results using the hexapod have shown that controllers designed using a decentralized single-strut design work well when compared to full multivariable methodologies.

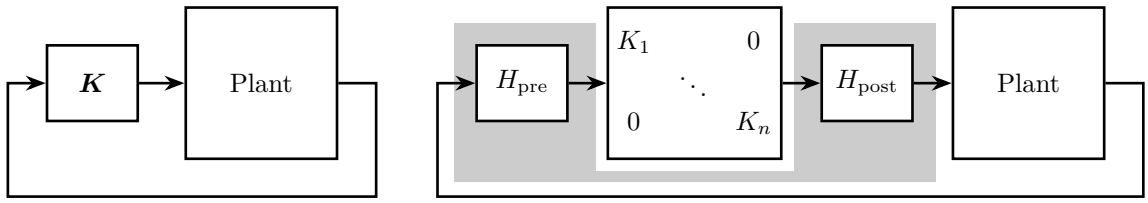

(a) Multivariable Control **(b)** Decoupling Control

Figure 3.15: Two strategies to control a multi-inputs-multi-outputs system. Use of a multivariable controller (a), or first decouple the plant with matrices, and then designing several single-input-single-output controllers (b)

- Explain the Jacobian matrix

When decoupling using the Jacobian matrix, the control can be performed in the frame of the struts (Figure 3.16a) or in the cartesian frame (Figure 3.16b).

Use of Multiple Sensors Often, both vibration control and position control is wanted. In that case, the use of multiple sensors can lead to improved performances.

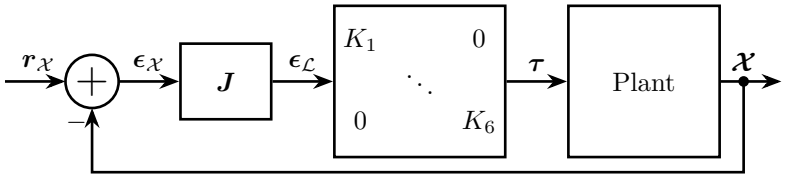

(a) Control in the frame of the struts

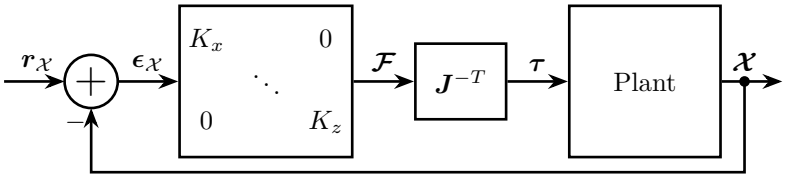

(b) Control in the cartesian frame

Figure 3.16: Two centralized control strategies. Express the position error in the frame of the struts and design one controller for each strut (a). Design one controller for each direction, and then map the forces and torques to each struts (b).

Sensors:

- collocated force (load cell) sensors
- collocated accelerometer
- displacement (eddy current)

Several strategies can be employed:

- HAC-LAC [37]–[41]
- Sensor Fusion [28], [42], [43]
- Two Sensor control: [28], [42]

Comparison between “two sensor control” and “sensor fusion” is given in [44].

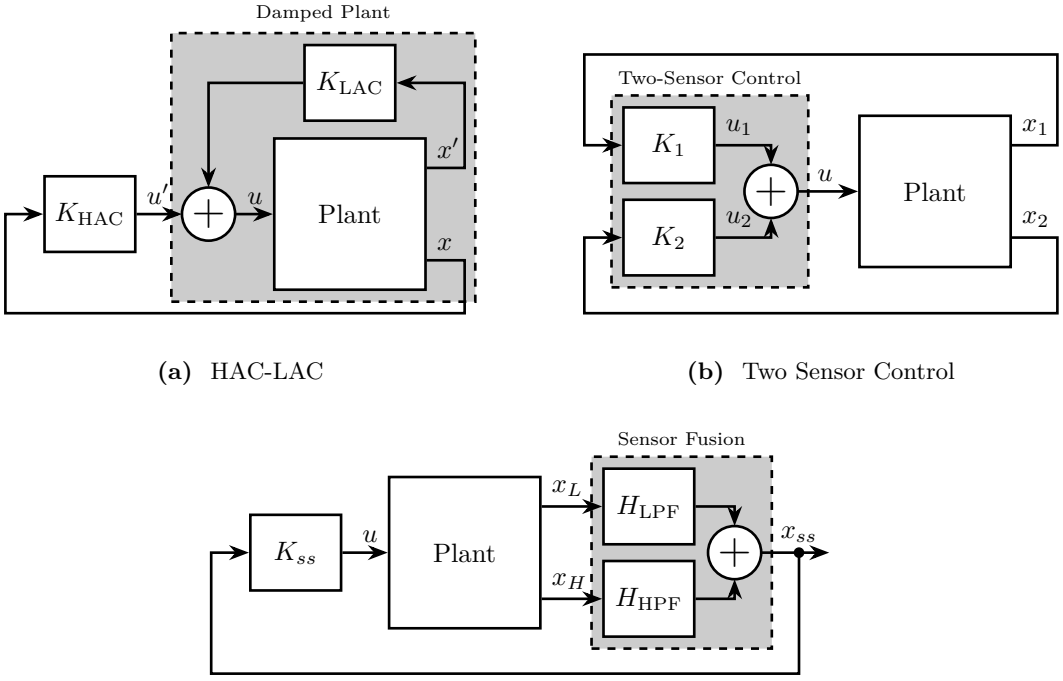

(a) HAC-LAC

(b) Two Sensor Control

(c) Sensor Fusion

Figure 3.17: Different control strategies when using multiple sensors. High Authority Control / Low Authority Control (a). Sensor Fusion (c). Two-Sensor Control (b)

4 Original Contributions

This thesis proposes several contributions in the fields of Control, Mechatronics Design and Experimental validation.

Active Damping of rotating mechanical systems using Integral Force Feedback [45], [46]

> his paper investigates the use of Integral Force Feedback (IFF) for the active damping of rotating mechanical systems. Guaranteed stability, typical benefit of IFF, is lost as soon as the system is rotating due to gyroscopic effects. To overcome this issue, two modifications of the classical IFF control scheme are proposed. The first consists of slightly modifying the control law while the second consists of adding springs in parallel with the force sensors. Conditions for stability and optimal parameters are derived. The results reveal that, despite their different implementations, both modified IFF control scheme have almost identical damping authority on the suspension modes.

Design of complementary filters using $\mathcal{H}_\infty$ Synthesis and sensor fusion [47] [48] [49]

- Several uses (link to some papers).
- For the NASS, they could be use to further improve the robustness of the system.

Multi-body simulations with reduced order flexible bodies obtained by FEA [31]

Combined multi-body / FEA techniques and experimental validation on a Stewart platform containing amplified piezoelectric actuators Super-element of amplified piezoelectric actuator / combined multibody-FEA technique, experimental validation on an amplified piezoelectric actuator and further validated on a complete stewart platform

> e considered sub-components in the multi-body model as *reduced order flexible bodies* representing the component's modal behaviour with reduced mass and stiffness matrices obtained from finite element analysis (FEA) models. These matrices were created from FEA models via modal reduction techniques, more specifically the *component mode synthesis* (CMS). This makes this design approach a combined multibody-FEA technique. We validated the technique with a test bench that confirmed the good modelling capabilities using reduced order flexible body models obtained from FEA for an amplified piezoelectric actuator (APA).

Robustness by design

- Design of a Stewart platform and associated control architecture that is robust to large plant uncertainties due to large variety of payload and experimental conditions.
- Instead of relying on complex controller synthesis (such as $\mathcal{H}_\infty$ synthesis or μ-synthesis) to guarantee the robustness and performance.
- The approach here is to choose an adequate architecture (mechanics, sensors, actuators) such that controllers are robust by nature.
- Example: collocated actuator/sensor pair => controller can easily be made robust
- This is done by using models and using HAC-LAC architecture

Mechatronics design Conduct a rigorous mechatronics design approach for a nano active stabilization system [50], [51]

Approach from start to finish:

- From first concepts using basic models, to concept validation
- Detailed design phase
- Experimental phase

Complete design with clear choices based on models. Such approach, while not new, is here applied This can be used for the design of future end-stations.

6DoF vibration control of a rotating platform Vibration control in 5DoF of a rotating stage To the author's knowledge, the use of a continuously rotating stewart platform for vibration control has not been proved in the literature.

Experimental validation of the Nano Active Stabilization System Demonstration of the improvement of the the positioning accuracy of a complex multi DoF (the micro-station) by several orders of magnitude (Section ...) using ...

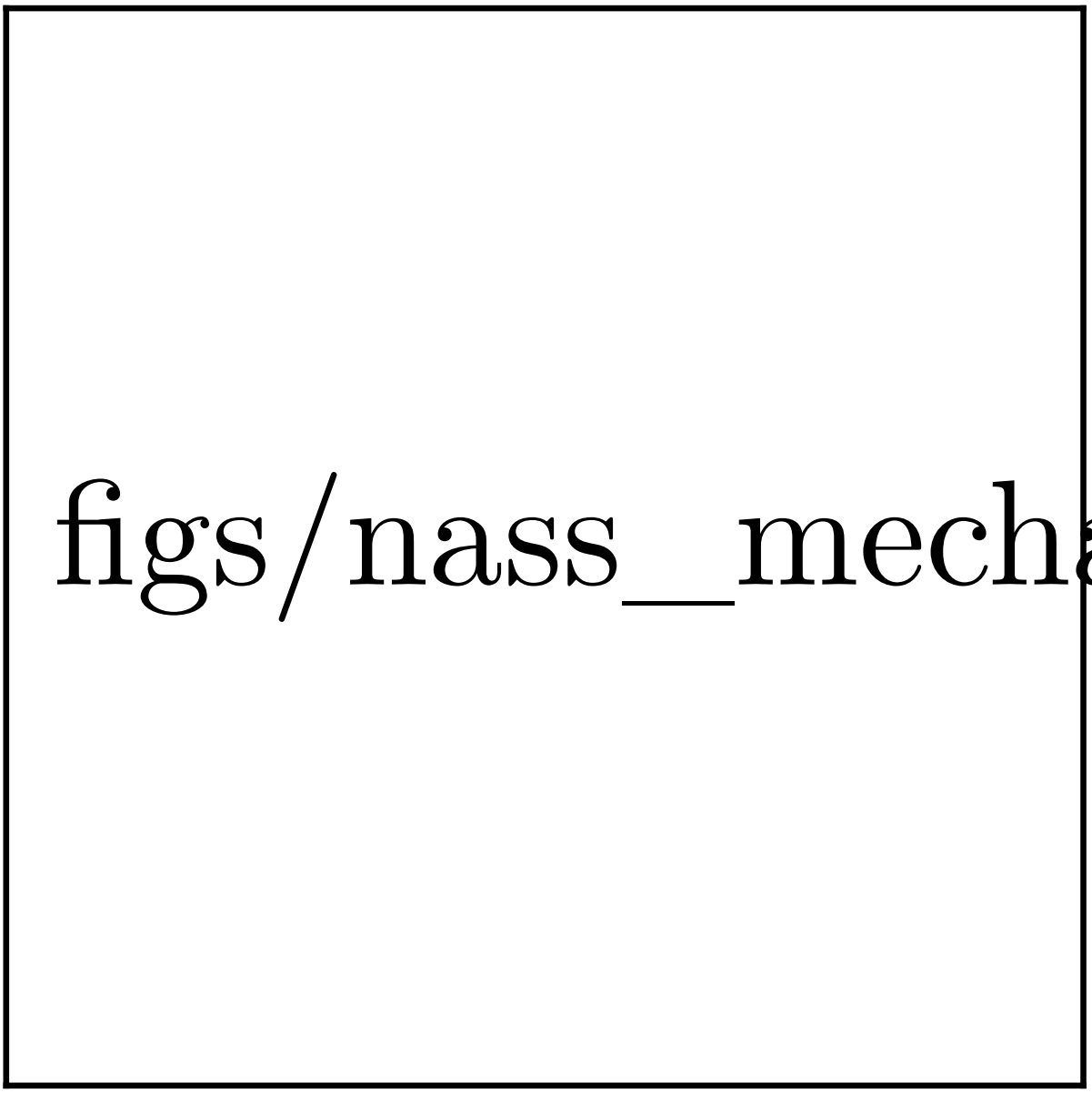

Figure 4.1: Overview of the mechatronic approach used for the Nano-Active-Stabilization-System

5 Thesis Outline - Mechatronics Design Approach

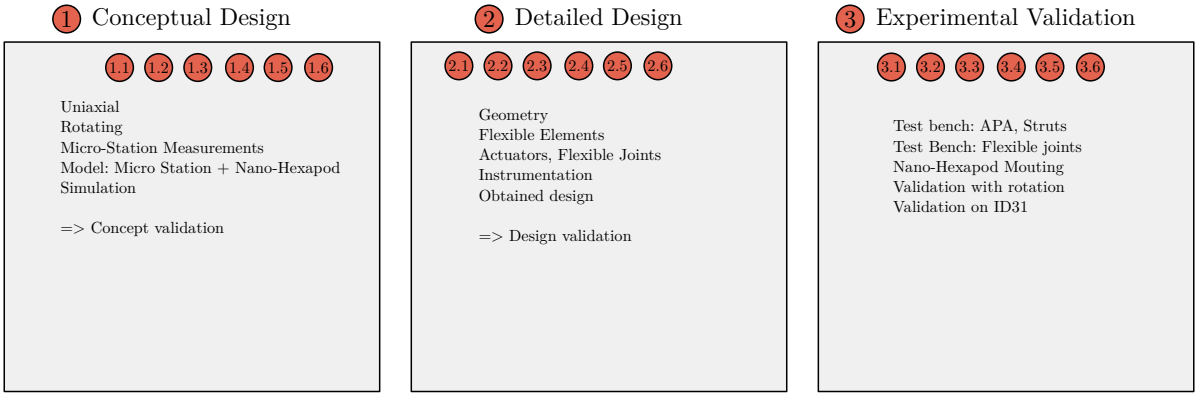

Figure 5.1: Overview of the sections

This thesis

- has a structure that follows the mechatronics design approach

Is structured in three chapters that corresponds to the three mains parts of the proposed mechatronics approach.

A brief overview of these three chapters is given bellow.

Conceptual design development

- Start with simple models for witch trade offs can be easily understood (uniaxial)
- Increase the model complexity if important physical phenomenon are to be modelled (cf the rotating model)
- Only when better understanding of the physical effects in play, and only if required, go for higher model complexity (here multi-body model)
- The system concept and main characteristics should be extracted from the different models and validated with closed-loop simulations with the most accurate model
- Once the concept is validated, the chosen concept can be design in mode details

Detailed design

- During this detailed design phase, models are refined from the obtained CAD and using FEM
- The models are used to assists the design and to optimize each element based on dynamical analysis and closed-loop simulations
- The requirements for all the associated instrumentation can be determined from a dynamical noise budgeting
- After converging to a detailed design that give acceptable performance based on the models, the different parts can be ordered and the experimental phase begins

Experimental validation

- It is advised that the important characteristics of the different elements are evaluated individually Systematic validation/refinement of models with experimental measurements
- The obtained characteristics can be used to refine the models
- Then, an accurate model of the system is obtained which can be used during experimental tests (for control synthesis for instance)

Bibliography

[1] P. Raimondi, N. Carmignani, L. R. Carver, *et al.*, "Commissioning of the hybrid multibend achromat lattice at the european synchrotron radiation facility," *Physical Review Accelerators and Beams*, vol. 24, no. 11, p. 110 701, 2021 (cit. on p. 4).

[2] V. Schoeppler, E. Reich, J. Vacelet, *et al.*, "Shaping highly regular glass architectures: A lesson from nature," *Science Advances*, vol. 3, no. 10, eaao2047, 2017 (cit. on p. 7).

[3] C. Sanchez-Cano, I. Romero-Canelón, Y. Yang, *et al.*, "Synchrotron x-ray fluorescence nanoprobe reveals target sites for organo-osmium complex in human ovarian cancer cells," *Chemistry - A European Journal*, vol. 23, no. 11, pp. 2512–2516, 2017 (cit. on pp. 7, 8).

[4] R. Barrett, R. Baker, P. Cloetens, *et al.*, "Reflective optics for hard x-ray nanofocusing applications at the esrf," *Synchrotron Radiation News*, vol. 29, no. 4, pp. 10–15, 2016 (cit. on p. 8).

[5] T. Hatsui and H. Graafsma, "X-ray imaging detectors for synchrotron and xfel sources," *IUCrJ*, vol. 2, no. 3, pp. 371–383, 2015 (cit. on p. 8).

[6] X. Huang, K. Lauer, J. N. Clark, *et al.*, "Fly-scan ptychography," *Scientific Reports*, vol. 5, no. 1, p. 9074, 2015 (cit. on p. 8).

[7] W. Xu, H. Xu, D. Gavrilov, *et al.*, "High-speed fly-scan capabilities for x-ray microscopy systems at nsls-ii," in *X-Ray Nanoimaging: Instruments and Methods VI*, Oct. 2023, nil (cit. on pp. 9, 17, 18).

[8] S. J. Leake, G. A. Chahine, H. Djazouli, *et al.*, "The nanodiffraction beamline id01/esrf: A microscope for imaging strain and structure," *Journal of Synchrotron Radiation*, vol. 26, no. 2, pp. 571–584, 2019 (cit. on p. 16).

[9] J. Wright, C. Giacobbe, and M. Majkut, "New opportunities at the materials science beamline at esrf to exploit high energy nano-focus x-ray beams," *Current Opinion in Solid State and Materials Science*, vol. 24, no. 2, p. 100 818, 2020 (cit. on p. 16).

[10] C. Riekel, M. Burghammer, and R. Davies, "Progress in micro- and nano-diffraction at the esrf id13 beamline," *IOP Conference Series: Materials Science and Engineering*, vol. 14, no. nil, p. 012 013, 2010 (cit. on p. 16).

[11] G. Martínez-Criado, J. Villanova, R. Tucoulou, *et al.*, "Id16b: A hard x-ray nanoprobe beamline at the esrf for nano-analysis," *Journal of Synchrotron Radiation*, vol. 23, no. 1, pp. 344–352, 2016 (cit. on p. 16).

[12] C. G. Schroer, M. Seyrich, M. Kahnt, *et al.*, "Ptynami: Ptychographic nano-analytical microscope at petra iii: Interferometrically tracking positions for 3d x-ray scanning microscopy using a ball-lens retroreflector," in *X-Ray Nanoimaging: Instruments and Methods III*, Sep. 2017 (cit. on pp. 17, 18).

[13] F. Villar, L. Andre, R. Baker, *et al.*, "Nanopositioning for the esrf id16a nano-imaging beamline," *Synchrotron Radiation News*, vol. 31, no. 5, pp. 9–14, 2018 (cit. on pp. 17–19).

[14] A. Schropp, R. Döhrmann, S. Botta, *et al.*, "Ptynami: Ptychographic nano-analytical microscope," *Journal of Applied Crystallography*, vol. 53, no. 4, pp. 957–971, 2020 (cit. on pp. 17, 18).

[15] E. Nazaretski, K. Lauer, H. Yan, *et al.*, "Pushing the limits: An instrument for hard x-ray imaging below 20 nm," *Journal of Synchrotron Radiation*, vol. 22, no. 2, pp. 336–341, 2015 (cit. on pp. 17–19).

[16] T. Stankevic, C. Engblom, F. Langlois, *et al.*, "Interferometric characterization of rotation stages for x-ray nanotomography," *Review of Scientific Instruments*, vol. 88, no. 5, p. 053 703, 2017 (cit. on pp. 17–19).

[17] C. Engblom *et al.*, "Nanoprobe results: Metrology & control in stacked closed-loop systems," in *Proc. of International Conference on Accelerator and Large Experimental Control Systems (ICALEPCS'17)*, JACoW, Jan. 2018 (cit. on pp. 17–19).

[18] E. Nazaretski, D. S. Coburn, W. Xu, *et al.*, "A new kirkpatrick-baez-based scanning microscope for the submicron resolution x-ray spectroscopy (srx) beamline at nsls-ii," *Journal of Synchrotron Radiation*, vol. 29, no. 5, pp. 1284–1291, 2022 (cit. on pp. 17–19).

[19] M. Holler, J. Raabe, R. Wepf, *et al.*, "Omny pin-a versatile sample holder for tomographic measurements at room and cryogenic temperatures," *Review of Scientific Instruments*, vol. 88, no. 11, p. 113 701, 2017 (cit. on pp. 17–19).

[20] M. Holler, J. Raabe, A. Diaz, *et al.*, "Omny-a tomography nano cryo stage," *Review of Scientific Instruments*, vol. 89, no. 4, p. 043 706, 2018 (cit. on pp. 17–19).

[21] J. Kelly, A. Male, N. Rubies, *et al.*, "The delta robot-a long travel nano-positioning stage for scanning x-ray microscopy," *Review of Scientific Instruments*, vol. 93, no. 4, nil, 2022 (cit. on pp. 17–19).

[22] R. R. Geraldes, G. B. Z. L. Moreno, F. R. Lena, *et al.*, "The high-dynamic cryogenic sample stage for sapoti/carnaúba at sirius/lnls," in *PROCEEDINGS OF THE 15TH INTERNATIONAL CONFERENCE ON X-RAY MICROSCOPY - XRM2022*, 2023, nil (cit. on pp. 17–19).

[23] J. Wang, Y.-c. K. Chen, Q. Yuan, *et al.*, "Automated markerless full field hard x-ray microscopic tomography at sub-50 nm 3-dimension spatial resolution," *Applied Physics Letters*, vol. 100, no. 14, p. 143 107, 2012 (cit. on pp. 17, 18).

[24] E. Nazaretski, H. Yan, K. Lauer, *et al.*, "Design and performance of an x-ray scanning microscope at the hard x-ray nanoprobe beamline of nsls-ii," *Journal of Synchrotron Radiation*, vol. 24, no. 6, pp. 1113–1119, 2017 (cit. on p. 18).

[25] H. Shinno, H. Yoshioka, and H. Sawano, "A newly developed long range positioning table system with a sub-nanometer resolution," *CIRP Annals*, vol. 60, no. 1, pp. 403–406, 2011 (cit. on p. 20).

[26] R. M. Schmidt, G. Schitter, and A. Rankers, *The Design of High Performance Mechatronics - Third Revised Edition*. Ios Press, 2020 (cit. on pp. 20, 22).

[27] Z. Du, R. Shi, and W. Dong, "A piezo-actuated high-precision flexible parallel pointing mechanism: Conceptual design, development, and experiments," *IEEE Transactions on Robotics*, vol. 30, no. 1, pp. 131–137, 2014 (cit. on p. 21).

[28] G. Hauge and M. Campbell, "Sensors and control of a space-based six-axis vibration isolation system," *Journal of Sound and Vibration*, vol. 269, no. 3-5, pp. 913–931, 2004 (cit. on pp. 21, 26).

[29] W. Monkhorst, "Dynamic error budgeting, a design approach," Ph.D. dissertation, Delft University, 2004 (cit. on pp. 20, 23).

[30] A. M. Rankers, "Machine dynamics in mechatronic systems: An engineering approach.," Ph.D. dissertation, University of Twente, 1998 (cit. on p. 22).

[31] P. Brumund and T. Dehaeze, "Multibody simulations with reduced order flexible bodies obtained by fea," in *MEDSI'20*, (Chicago, USA), ser. Mechanical Engineering Design of Synchrotron Radiation Equipment and Instrumentation, JACoW Publishing, 2021 (cit. on pp. 22, 28).

[32] L. Jabben, "Mechatronic design of a magnetically suspended rotating platform," Ph.D. dissertation, Delft University, 2007 (cit. on p. 23).

[33] A. Okyay, "Mechatronic design, dynamics, controls, and metrology of a long-stroke linear nanopositioner," Ph.D. dissertation, University of Waterloo, 2016 (cit. on p. 23).

[34] C. Collette, S. Janssens, and K. Artoos, "Review of active vibration isolation strategies," *Recent Patents on Mechanical Engineeringe*, vol. 4, no. 3, pp. 212–219, 2011 (cit. on p. 23).

[35] S. Chesné, A. Milhomem, and C. Collette, "Enhanced damping of flexible structures using force feedback," *Journal of Guidance, Control, and Dynamics*, vol. 39, no. 7, pp. 1654–1658, 2016 (cit. on p. 24).

[36] D. Thayer, M. Campbell, J. Vagners, and A. von Flotow, "Six-axis vibration isolation system using soft actuators and multiple sensors," *Journal of Spacecraft and Rockets*, vol. 39, no. 2, pp. 206–212, 2002 (cit. on p. 25).

[37] Z. J. Geng, G. G. Pan, L. S. Haynes, B. K. Wada, and J. A. Garba, "An intelligent control system for multiple degree-of-freedom vibration isolation," *Journal of Intelligent Material Systems and Structures*, vol. 6, no. 6, pp. 787–800, 1995 (cit. on p. 26).

[38] C. Wang, X. Xie, Y. Chen, and Z. Zhang, "Investigation on active vibration isolation of a stewart platform with piezoelectric actuators," *Journal of Sound and Vibration*, vol. 383, pp. 1–19, Nov. 2016 (cit. on p. 26).

[39] X. Li, J. C. Hamann, and J. E. McInroy, "Simultaneous vibration isolation and pointing control of flexure jointed hexapods," in *Smart Structures and Materials 2001: Smart Structures and Integrated Systems*, Aug. 2001 (cit. on p. 26).

[40] H. Pu, X. Chen, Z. Zhou, and X. Luo, "Six-degree-of-freedom active vibration isolation system with decoupled collocated control," *Proceedings of the Institution of Mechanical Engineers, Part B: Journal of Engineering Manufacture*, vol. 226, no. 2, pp. 313–325, 2011 (cit. on p. 26).

[41] X. Xie, C. Wang, and Z. Zhang, "Modeling and control of a hybrid passive/active stewart vibration isolation platform," in *INTER-NOISE and NOISE-CON Congress and Conference Proceedings*, Institute of Noise Control Engineering, vol. 255, 2017, pp. 1844–1853 (cit. on p. 26).

[42] D. Tjepkema, "Active hard mount vibration isolation for precision equipment [ph. d. thesis]," Ph.D. dissertation, 2012 (cit. on p. 26).

[43] D. Tjepkema, J. van Dijk, and H. Soemers, "Sensor fusion for active vibration isolation in precision equipment," *Journal of Sound and Vibration*, vol. 331, no. 4, pp. 735–749, 2012 (cit. on p. 26).

[44] M. A. Beijen, D. Tjepkema, and J. van Dijk, "Two-sensor control in active vibration isolation using hard mounts," *Control Engineering Practice*, vol. 26, pp. 82–90, 2014 (cit. on p. 26).

[45] T. Dehaeze and C. Collette, "Active damping of rotating platforms using integral force feedback," in *Proceedings of the International Conference on Modal Analysis Noise and Vibration Engineering (ISMA)*, 2020 (cit. on p. 28).

[46] T. Dehaeze and C. Collette, "Active damping of rotating platforms using integral force feedback," *Engineering Research Express*, Feb. 2021 (cit. on p. 28).

[47] T. Dehaeze, M. Vermat, and C. Collette, "Complementary filters shaping using $\mathcal{H}_\infty$ synthesis," in *7th International Conference on Control, Mechatronics and Automation (ICCMA)*, 2019, pp. 459–464 (cit. on p. 28).

[48] M. Verma, T. Dehaeze, G. Zhao, J. Watchi, and C. Collette, "Virtual sensor fusion for high precision control," *Mechanical Systems and Signal Processing*, vol. 150, p. 107 241, 2020 (cit. on p. 28).

[49] T. T. L. Tsang, T. G. F. Li, T. Dehaeze, and C. Collette, "Optimal sensor fusion method for active vibration isolation systems in ground-based gravitational-wave detectors," *Classical and Quantum Gravity*, vol. 39, no. 18, p. 185 007, 2022 (cit. on p. 28).

[50] T. Dehaeze, M. M. Mattenet, and C. Collette, "Sample stabilization for tomography experiments in presence of large plant uncertainty," in *MEDSI'18*, (Paris, France), ser. Mechanical Engineering Design of Synchrotron Radiation Equipment and Instrumentation, Geneva, Switzerland: JACoW Publishing, Dec. 2018, pp. 153–157 (cit. on pp. 19, 29).

[51] T. Dehaeze, J. Bonnefoy, and C. Collette, "Mechatronics approach for the development of a nano-active-stabilization-system," in *MEDSI'20*, (Chicago, USA), ser. Mechanical Engineering Design of Synchrotron Radiation Equipment and Instrumentation, JACoW Publishing, 2021 (cit. on pp. 19, 29).